

## Effect of over- and under-burden on time-lapse CSEM monitoring capabilities

Arash JafarGandomi\* and Andrew Curtis, School of GeoSciences, The University of Edinburgh, Kings Buildings, Edinburgh EH9 3JW, UK

### Summary

We investigate the impact of over- and under-burden resistivity structure on the time-lapse monitoring of the subsurface reservoirs with CSEM method. We show that even the introduction of a single, thin, high-resistivity layer in the over-burden may effectively remove our monitoring capability. Such a layer even in the under-burden can affect our monitoring capability significantly. In the over-burden the impact of the high-resistivity layer decreases as the high-resistivity layer gets closer to the reservoir, while the opposite is true when the high-resistivity layer is in the under-burden. The effect of the high-resistivity layer is negligible only if located deeper than two times the reservoir burial depth.

### Introduction

For decades the seismic-reflection method has been considered as the most appropriate geophysical method to explore for offshore hydrocarbon reservoirs due to its high spatial resolution. However, distinguishing between different hydrocarbon fluids is still a major challenge for seismic analysis techniques (e.g., Thirud 2002). Strong variation of the resistivity of reservoir rocks with partial fluid saturation (e.g., proportions in a gas and brine composite) has inspired the application of electrical and electromagnetic methods in geophysical exploration and monitoring. Although this sensitivity is supported by theoretical relations (e.g., Archie, 1942) and laboratory measurements (e.g., Stalheim et al., 1999), reliable estimation of its value in the field remains a challenge. It is possible to measure resistivity of geological formations with high accuracy using well-based techniques. However, these measurements are spatially limited to the few centimetres around the borehole, and the cost of drilling a borehole is high.

Recently, the marine controlled-source electromagnetic method (CSEM) has been tested for hydrocarbon exploration and subsurface reservoir monitoring. Um & Alumbaugh (2007) examined the underlying physics of the CSEM method. They demonstrated that the efficiency of marine CSEM for detecting high-resistivity thin layers at depth is strongly dependent on the source-receiver geometrical configurations and source-frequency range.

A developing area of application of CSEM is monitoring of offshore CO<sub>2</sub> storage sites. Sequestration of CO<sub>2</sub> captured at power plants into geological formations is potentially a practical approach towards the reduction of greenhouse

gases in the atmosphere. Even though CO<sub>2</sub> injection into brine saturated sandstones significantly increases the resistivity of rocks, detectability of these changes remains a challenge particularly in the case of offshore storage sites. There have been several studies on the feasibility of monitoring CO<sub>2</sub> storages by electrical methods (e.g., Christensen et al., 2006; Gasperikova et al., 2006; Kiessling et al., 2010). Orange et al. (2009) examined the applicability of the marine CSEM method to the reservoir-monitoring problem by analyzing representative 2D models. Their studies show that CSEM responses exhibit small but measurable changes when 10% of the resistive reservoir (e.g., gas filled reservoir) is replaced by conductive pore fluids.

A major challenge for geophysical monitoring is the existence of very high resistivity layers. Such contrasting layers act to reduce the CSEM sensitivity to CO<sub>2</sub> saturation. The geology of the CO<sub>2</sub> storage site dictates the magnitude of signal that is in principle measurable given any injection scenario. To investigate this effect we apply a forward modelling approach to predict the time-lapse CSEM response of a range of 1D subsurface CO<sub>2</sub> reservoir models. Each model consists of a storage formation and a high-resistivity layer in either the lower resistivity over- or under-burden. We introduce a detectability parameter based on the time-lapse CSEM response of the subsurface model for a range of frequencies and source-receiver offsets. Variation of the detectability parameter for different subsurface models indicates the impact of the site geology on the reservoir monitorability.

### Effect of CO<sub>2</sub> injection on reservoir rock resistivity

Laboratory measurements are used to analyse the effect of CO<sub>2</sub> on the electrical resistivity of rocks. Mayer (2001) measured the effect of injecting CO<sub>2</sub> into brine on the rock resistivity. His results show that the effect depends on the brine salinity and pore pressure. Nakatsuka et al. (2009) studied the effect of CO<sub>2</sub> on the bulk resistivity of rocks and proposed a procedure for quantifying injected CO<sub>2</sub> from resistivity measurement in saline aquifer storage based on laboratory experiments.

In the CASSEM (CO<sub>2</sub> Aquifer Storage Site Evaluation and Monitoring) project, the effect of CO<sub>2</sub> injection on the electrical resistivity of analogue reservoir sandstones was also examined by conducting laboratory experiments (Fisher et al., 2010). A sandstone sample from a saline aquifer in the North Sea with porosity of 20.15 % and permeability of 99.25 mD was tested with electromagnetic

## Effect of over/under burden on time-lapse CSEM

(EM) measurements. The EM properties of the sample were measured under four differential pressures of 1000, 2000, 3000 and 4000 psi and for 100% brine-saturated sample and partially CO<sub>2</sub> flooded samples with 58.5% and 81.5% CO<sub>2</sub> saturation. Temperature and pressure of the injected supercritical CO<sub>2</sub> were 40 °C and 2000 psi, respectively. Figure 1 shows the corresponding measured resistivities at the frequency of 50 Hz versus differential stress. The experimental results indicate that with 81.5% CO<sub>2</sub> saturation the resistivity of the sample increases by about an order of magnitude than the result at 0% saturation. However, the sample's resistivity presents relatively little sensitivity to the differential stress, especially at lower CO<sub>2</sub> saturations.

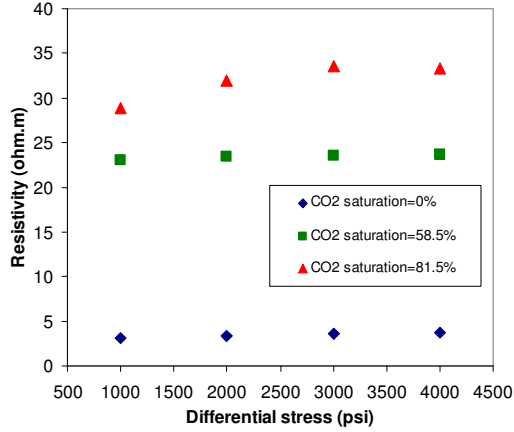


Figure 1: Resistivity data measured from the analogue reservoir sandstone at different differential stresses and CO<sub>2</sub> saturations.

From hereon, the results of the laboratory measurements are used to create 1D subsurface resistivity models for the CO<sub>2</sub> reservoir to assess the detectability of its resistivity changes.

### Time-lapse marine CSEM

Time-lapse geophysical monitoring is an efficient way to track changes in subsurface reservoirs. Changes in the petrophysical properties of a reservoir are detectable as long as the magnitude of the measured geophysical signal is above the noise level ( $NL$ ). In the case of CSEM, magnitude of the measured signal depends on the site geology, the frequency, and the source-receiver offset. In order to estimate detectability of the changes in the reservoir we define the following detectability parameter

$$M(\chi) = \frac{1}{mn} \sum_{ij} \frac{|\chi_{ij}^{CO_2} - \chi_{ij}^0|}{NL}, \quad (1)$$

where  $\chi$  is the vertical or horizontal electric-field component, subscripts  $i$  and  $j$  represent the frequency and

the source-receiver offsets, respectively,  $m$  and  $n$  are the total number of the frequency and the source-receiver offsets, respectively, and  $\chi_{ij}^{CO_2}$  and  $\chi_{ij}^0$  are the calculated electric-field components after and before injecting CO<sub>2</sub> into the reservoir, respectively. Since the  $NL$  of the source-receiver system plays an important role in the detectability, the detectability parameter is normalised by  $NL$ .

In order to illustrate the effect of site geology on detectability, we consider three different models of storage formations. The first model is a simple model of a storage formation with the resistivity of 3 ohm.m (analogous to the measured resistivity of the brine-saturated sample) and thickness of 100 m at a depth of 1000 m below the seabed, within a background medium consisting of a lower half-space with the resistivity of 1 ohm.m, an overlaying sea water layer with the resistivity of 0.3 ohm.m and the thickness of 1000 m, and upper half-space representing air with resistivity of  $1 \times 10^{12}$  ohm.m (Figure 2a). The second model is identical to the first except that it has a 20 m thick relatively high-resistivity (500 ohm.m) layer at 800 m depth below the seabed in the over-burden (Figure 2b). The third is also identical to the first except that it has a 20 m thick relatively high-resistivity (500 ohm.m) layer at 1200 m depth below the seabed in the under-burden (Figure 2c). We model the CSEM responses for a single receiver located on the seabed for a series of inline horizontal electric dipole (HED) transmitters from 0 to 20 km horizontal position at 50 m above the seafloor. We use the Occam1DCSEM code of Key (2009) to calculate the synthetic responses.

We assume that the CO<sub>2</sub> saturation in the reservoir is 58.5% and according to the laboratory results in Figure 1 the resistivity of the reservoir increases to 23 ohm.m after injecting CO<sub>2</sub>. To see the effect of CO<sub>2</sub> injection on the time-lapse CSEM monitoring, we calculate the CSEM responses of the three models before and after injecting CO<sub>2</sub> for a range of frequencies from 0.1 to 10 Hz, and for transmitter-receiver offsets from 0 to 20 km. Figure 2 (right panels) show the base-10 logarithm of the detectability parameter for the radial horizontal electric-field responses of the models, as a function of offset and frequency. The  $NL$  is assumed to be  $10^{-15}$  V/Am<sup>2</sup>.

Figure 2 demonstrates which combination of the offsets and frequencies are appropriate for detecting resistivity changes in each simple storage formation. Right panels in Figure 2 can be used to design CSEM experiment. For an efficient CSEM experiment the trade-off between frequency and transmitter-receiver offset has to be taken into account. It can be seen from Figure 2b that even the introduction of a single, thin, high-resistivity layer in the over-burden may effectively remove our monitoring capability using the

## Effect of over/under burden on time-lapse CSEM

CSEM method. Figure 2c implies that the presence of a single, thin, high-resistivity layer even in the *under*-burden can also affect our monitoring capability. The presence of a thin high-resistivity layer in the over- or under-burden reduces the strength of the time-lapse changes in the CSEM signal. However, in both cases presence of the high-resistivity layer increases the maximum offset where the signal is detectable. This is due to greater average resistivity of the model in the presence of high-resistivity layers, which leads to less attenuation of the electric-current with distance.

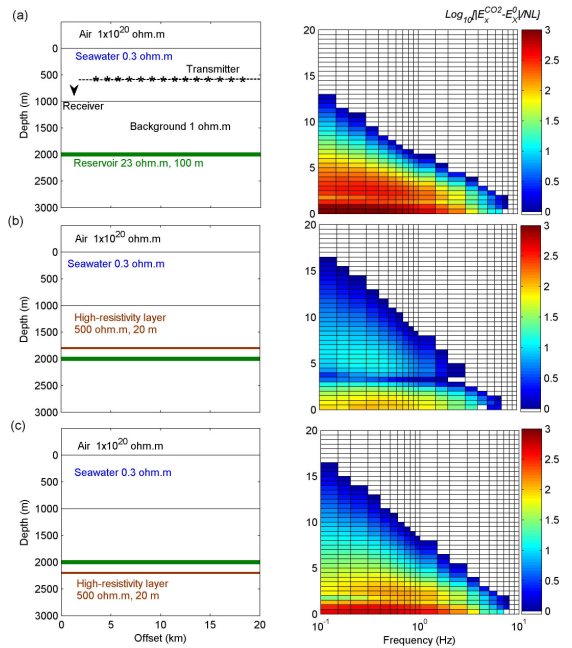


Figure 2. Three structure models (left) used for calculating the detectability parameter of the models (right) after injecting  $\text{CO}_2$ . Colour scales show base-10 logarithm of the detectability parameter of the horizontal electric-field components for each frequency-offset pair.

To better understand the effect of the high-resistivity layer on the detectability we investigate the direction of electric-current induced by HED at 1 Hz. Figure 3 is a snap-shot of the electric-current for the model in Figure 2b zoomed around the high-resistivity layer and the reservoir. In this figure white arrows indicate direction of the electric-current. Direction of the current in the high-resistivity layer is vertical; thus causes the current to flow parallel to the interfaces with phase reversal above and below the high-resistivity layer. Blocking of the vertical current in the high-resistivity layer which lead to discontinuity in the horizontal current and phase reversal above and below its interfaces (e.g., Um & Alumbaugh, 2007) are the likely reasons for detectability reduction.

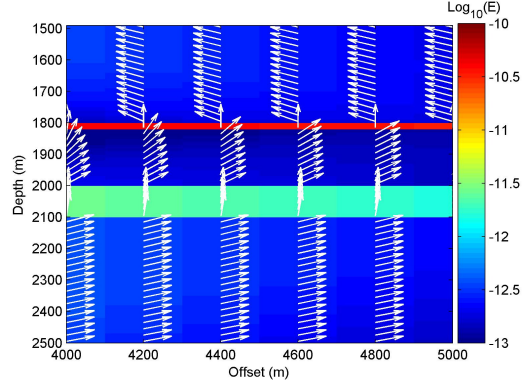


Figure 3. Snap shot of the electric-current flow direction around the high-resistivity layer and the  $\text{CO}_2$  saturated reservoir induced by HED at 1 Hz. The colour scale indicates amplitude of the electric-field.

In order to investigate the influence of distance of the high-resistivity layer from the reservoir on the detectability parameter, we move the high-resistivity layer vertically from just below the seabed to 3000 m depth below the seabed in 200 m steps, and at each step we calculate the detectability parameter for horizontal and vertical components of the electric-field,  $E_x$  and  $E_z$ , respectively. In this case we assume the same  $NL$  for  $E_x$  and  $E_z$ , however in practice the vertical field measurements on current systems are generally more contaminated with instrumental noise than the horizontal components.

Figure 4 indicates that in the over-burden as the high-resistivity layer gets closer to the reservoir its effect on  $M(\chi)$  decreases while this is opposite when the high resistivity layer is in the under-burden. In other words, the deeper the high-resistivity layer, the less effect it has on detectability. Both  $M(E_x)$  and  $M(E_z)$  are asymptotic to their corresponding values for the homogeneous background only at about 1000 m below the reservoir. In other words, a resistive layer anywhere closer to the reservoir than 1 km decreases the efficiency of the CSEM survey.

Key (2009) examined the effect of multiple high-resistivity layers on the detectability of a hypothetical hydrocarbon reservoir with resistivity of 100 ohm.m at 1000 m depth below the seabed with marine CSEM. Key showed that the overlying high-resistivity layers have no noticeable effect on the detection of the deeper reservoir. Note that in Key's modelling the resistivity of overlying high-resistivity layers are less than the resistivity of the reservoir. We calculate  $M(\chi)$  for the models in Figure 2b and 2c for a range of resistivity values (1 ohm.m- 10000 ohm.m) for the

## Effect of over/under burden on time-lapse CSEM

high-resistivity layers. Figure 5 shows the calculated detectability parameters with respect to the normalised resistivity of the high-resistivity layer ( $\rho_{high} / \rho_{CO2}$ , where  $\rho_{CO2}$  and  $\rho_{high}$  are the resistivity of the CO<sub>2</sub> saturated reservoir and the high-resistivity layer, respectively). This figure implies that in these cases the reservoir monitorability is strongly affected by the high-resistivity layer when the resistivity of this layer is greater than 20% of the reservoir resistivity. Such situation may often occur in the case of multilayer storage formations.

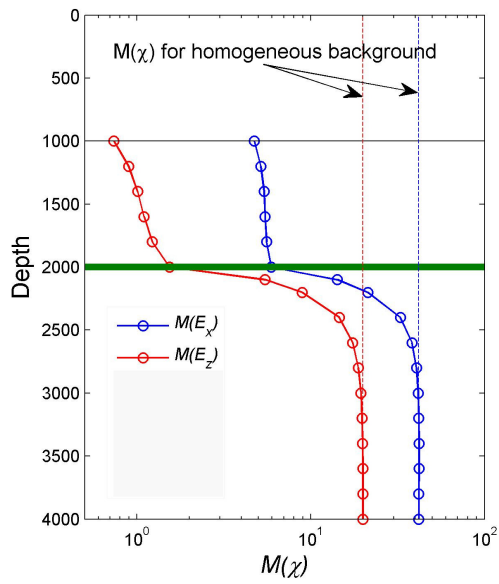


Figure 4. Variation of the detectability parameters for  $E_x$  and  $E_z$  with respect to the depth of the thin (20 m thick) high-resistivity (500 ohm.m) layer. Vertical dashed lines represent the corresponding detectability parameters for the homogeneous background (in the absence of the high-resistivity layer).

The main lesson from this section, however, is that the potential effectiveness of the CSEM monitoring method must be assessed in a site-by-site basis. This will require significant prior information about the conductivity structure of the reservoir, over-burden and under-burden. Off course, performing EM monitoring from borehole wells may reduce the susceptibility of the methods to surrounding high-resistivity layers, but this susceptibility will never be removed. This work also implies that the *under*-burden must be assessed in order to estimate monitorability of a potential reservoir, something not usually considered in site evaluation.

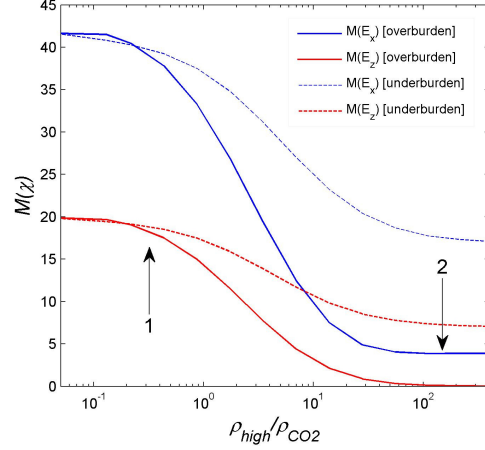


Figure 5. Variation of the detectability parameters versus normalised resistivity of the high-resistivity layer located in the over- and under-burden (solid and dashed lines, respectively). 1- Region studied by Key (2009); 2- region studied herein.

## Conclusion

We demonstrate the effect of over- and under-burden resistivity structure on the monitorability of subseafloor CO<sub>2</sub> reservoirs by marine CSEM. We analysed the sensitivity of time-lapse detectability of changes in the reservoir to a single 20 m thick, high-resistivity (500 ohm.m) layer in the over- and under-burden using a repeated forward modelling approach. Results show that monitorability of the subsurface CO<sub>2</sub> reservoirs with CSEM is strongly affected by such high-resistivity layers. The impact of the high-resistivity layer on the detectability of the changes in the reservoir with CSEM is not negligible unless its depth is greater than two times the reservoir burial depth, or its resistivity is less than 20% of the reservoir resistivity.

## Acknowledgments

The research related to this paper has been carried out within the CASSEM project, which is a project supported by the Technology Strategy Board. The authors wish to acknowledge the support of, the TSB and the EPSRC and the project industry partners; AMEC, Marathon, Schlumberger, Scottish Power, and Scottish and Southern Energy, and the academic partners; British Geological Survey, Heriot-Watt University, University of Edinburgh, and the University of Manchester. We also thank Quentin Fisher and his colleagues at the University of Leeds for providing us with the laboratory measurement.

## Reference

- Archie, G.E., 1942. The electrical resistivity log as an aid in determining some reservoir characteristics, *Transaction of American Institute of Mining, Metallurgical, and Petroleum Engineers*, 146, 54–62.
- Christensen N.B., Sherlock, D. and Dodds, K., 2006, Monitoring CO<sub>2</sub> injection with cross-hole electrical resistivity tomography, 37, 44-49.
- Constable, S., and C. J. Weiss, 2006, Mapping thin resistors and hydrocarbons with marine EM methods: Insights from 1D modeling: *Geophysics*, 71, no. 2, G43–G51.
- Fisher, Q. J., Martin, J., Grattoni, C., Angus, D. Guise, P., 2010, Ultrasonic velocity and electromagnetic property analysis of sandstone samples with varying brine and supercritical CO<sub>2</sub> saturations, British Geological Survey, CASSEM project report.
- Gasperikova, E., and M. Hoversten, 2006, A feasibility study of non-seismic geophysical methods for monitoring geologic CO<sub>2</sub> sequestration: *The Leading Edge*, 25, 1282–1288.
- Key, K., 2009, 1D inversion of multicomponent, multifrequency marine CSEM data: Methodology and synthetic studies for resolving thin high-resistivity layers: *Geophysics*, 74, no. 2, F9–F20.
- Kiessling, D., Schmidt-Hattenbergera, C., Schuetta, H., Schilling, F.,c, Kruegera, K., Schoebela, B., Danckwardtd, E., Kummerowa, J., and the CO<sub>2</sub>SINK Group, 2010, Geoelectrical methods for monitoring geological CO<sub>2</sub> storage: First results from cross-hole and surface–downhole measurements from the CO<sub>2</sub>SINK test site at Ketzin (Germany), *International Journal of Greenhouse Gas Control*, 4, 816–826.
- Myer, L.R. (2001): Laboratory Measurement of Geophysical Properties for Monitoring CO<sub>2</sub> Sequestration, *Proceedings, First National Symposium on Carbon Sequestration*, U. S. National Energy Technology Laboratory, Washington DC.
- Nakatsuka, Y., Xue, Z., Yamada, Y., and Matsuoka, T., 2009, Experimental study on monitoring and quantifying of injected CO<sub>2</sub> from resistivity measurement in saline aquifer storage, *Energy Procedia*, 1, 2211-2218.
- Orange, A., Key, K., and Constable, S., 2009, The feasibility of reservoir monitoring using time-lapse marine CSEM, *Geophysics*, 74, F21–F29.
- Stalheim, S.O., Eidesmo, T., Rueslatten, H., 1999, Influence of wettability on water saturation modelling, *Journal of Petroleum Science and Engineering*, 24, 243–253.
- Thirud, Å., 2002, EMGS article: *Scandinavian Oil-Gas Magazine*, Issue 3/4, 8–9.
- Um, E. S., and Alumbaugh, D. L., 2007, Marine Controlled-Source Electromagnetic Methods On the physics of the marine controlled-source electromagnetic method: *Geophysics*, 72, no. 2, WA13-WA26.